Fast relaxations in foam

Kapilanjan Krishan,[1,2] Ahmed Helal,[1] Reinhard Höhler,[1] and Sylvie Cohen-Addad[1,*]
[1]*Laboratoire de Physique des Matériaux Divisés et des Interfaces, FRE 3300 CNRS, Université Paris-Est, 5 Bd Descartes, Champs-sur-Marne, 77454 Marne-la-Vallée Cedex 2, France*
[2]*School of Physical Sciences, Jawaharlal Nehru University, New Delhi 110067, India*
(Received 9 December 2009; revised manuscript received 6 April 2010; published 23 July 2010)

Aqueous foams present an anomalous macroscopic viscoelastic response at high frequency, previously shown to arise from collective relaxations in the disordered bubble packing. We demonstrate experimentally how these mesoscopic dynamics are in turn tuned by physico-chemical processes on the scale of the gas-liquid interfaces. Two specific local dissipation processes are identified, and we show how the rigidity of the interfaces selects the dominant one, depending on the choice of the surfactant.

DOI: 10.1103/PhysRevE.82.011405 PACS number(s): 83.80.Iz, 82.70.Rr, 83.60.Bc

I. INTRODUCTION

Soft glassy complex fluids such as aqueous foams, concentrated emulsions or pastes are amorphous close packings of bubbles, droplets or particles with dynamics at multiple length and time scales [1–5]. The viscoelastic response of these materials exhibits an anomalous dissipation at high frequency. It has been explained as the consequence of relaxations in weak regions, expected to be a generic feature of randomly packed bubble, droplet or particle assemblies [4]. These mesoscopic dynamics are in turn governed by a fundamental characteristic relaxation frequency [4]. It depends on processes at the scale of the microstructure which have so far not been identified, but which a full theory of viscoelasticity for any soft glassy material must capture. Here, we focus on aqueous foams, chosen as a model system, and present experimental evidence providing the missing link between mesoscopic viscoelastic relaxation dynamics and local physico-chemical processes.

Aqueous foam is a concentrated dispersion of bubbles in a surfactant solution. Even though it consists only of fluids, it behaves like a linear elastic solid when subjected to sufficiently small deformations [6]. Since this elasticity arises from the strain induced variation of interfacial energy, the shear modulus G scales, for a given gas volume fraction, with the average bubble diameter d and surface tension T as [7]:

$$G \propto T/d. \tag{1}$$

The linear stress response to an oscillatory shear of frequency f is described by the complex shear modulus $G^*(f) = G'(f) + iG''(f)$. In foams, previous experiments and numerical simulations have evidenced two slow relaxation processes, dominant typically at frequencies below 1 Hz. A Maxwell relaxation driven by coarsening-induced bubble rearrangements [2,3,8] and a process, coupled to interfacial rheology, that arises from the dynamic adhesion between adjacent bubbles [3,9]. At high frequency, the modulus G^* in foams and emulsions presents an anomalous increase that scales with $\sqrt{f}$ [2,4,10]. It has been attributed to collective bubble relaxations in mesoscopic weak regions where the elastic restoring force is small in a particular shear direction, determined by the local disorder [4]. The macroscopic response is modeled as that of an elastic matrix of modulus G, in which anisotropic weak regions are dispersed. Their random orientation modulates their mechanical coupling to macroscopic shear of a given direction and therefore gives rise to a spectrum of relaxation times. Furthermore, the liquid viscosity is predicted to yield an additional contribution to G^*, dominant at high frequency, expressed as $2\pi i \eta_\infty f$. Finally, neglecting the slow relaxations, the following generic viscoelastic behavior is predicted [4]:

$$G^*(f) = G(1 + \sqrt{if/f_c}) + 2\pi i \eta_\infty f. \tag{2}$$

The characteristic viscoelastic relaxation frequency f_c of the weak regions is set by the interplay between an elastic restoring force and a viscous friction opposed to the shear motion, respectively characterized by a storage modulus g, assumed to scale as T/d, and an effective viscosity η_{eff} [4],

$$f_c = g/\eta_{eff}. \tag{3}$$

η_{eff} is predicted to differ from the viscosity of the foaming liquid, η, by a strain concentration factor, estimated as the ratio of bubble size d and film thickness δ.

However, Buzza *et al.* pointed out many other possible fast local relaxation processes involving convective or diffusive surfactant transport coupled to dissipative bulk flows [11]. These processes depend on interfacial rigidity, defined as the resistance offered by the gas-liquid interfaces to any motion within the surface [12] and previously found to control foam drainage [13] and stationary flow [14]. Interfacial rigidity is characterized by the complex surface dilatational modulus $E_D^* = E_S + iE_L$ that expresses the change of surface tension upon surface area variation.

II. EXPERIMENTAL METHODS

A. Rheometry

To identify the dominant physico-chemical processes which set f_c, we measure how the complex shear modulus G^* of foams depends on surface dilatational modulus, bulk liquid viscosity and bubble size, for frequencies between 1 Hz

*Author to whom correspondence should be addressed.

TABLE I. Foaming solution properties at $(21\pm1)\,^{\circ}$C. The viscosity η is measured using a capillary tube. The surface tension T and the surface dilatational modulus E_D^* are measured using a Teclis interfacial tensiometer with a bubble in air, oscillating at a frequency $f=0.1$ Hz with an area amplitude variation of 6.7%. The surface viscosity κ is deduced from the loss modulus E_L assuming Newtonian behavior: $\kappa = E_L/2\pi f$.

System	η (mPa s)	T (mN/m)	E_s (mN/m)	κ (g/s)	Interfacial type
Gillette foam (normal regular)	1.9	28.6	67	307	Rigid
SLES 40% Glycerol	3.7	33.3	≤ 10	≤ 10	
SLES 50% Glycerol	6.0	33.7	≤ 10	≤ 10	Mobile
SLES 60% Glycerol	10.8	34.4	20	30	

and 80 Hz. For foams, this range is inaccessible with most commercial rheometers because the inertia of the instrument strongly dominates over the sample response. We therefore use a custom built rheometer; it is a sliding plate device [15] where the sample is sheared between two rough horizontal parallel plates of large surface area (70×100 mm) held at a distance of either 3.9 mm or 4.9 mm. The upper plate oscillates horizontally at a given amplitude and frequency f. The amplitudes and phases of this displacement and of the shear stress exerted by the sample on the fixed lower plate are measured using two lock-in amplifiers. We deduce an apparent complex shear modulus of the foam from the ratio of measured stress and strain, and calculate the true modulus G^* by taking into account inertial forces within the sample [16]. To characterize the viscoelastic foam response, we perform frequency sweeps in the range 1 Hz$<f<$80 Hz, at constant imposed strain amplitude chosen in the range between 0.0018 and 0.0026 where the measured response is linear. Since G^* is found to be independent of the gap width, we conclude that there is no wall slip. Evaporation is prevented by saturating the air in contact with the free sample surfaces with water vapor.

B. Foam samples

We study two foams of the same gas volume fraction whose interfacial rheological properties strongly differ, Gillette shaving foam (Normal Regular) with rigid interfaces [14] and a foam with mobile interfaces, based on a mixed surfactant aqueous glycerol solution [17]. It is denoted SLES (cf. Table I) and contains Sodium Lauryl-dioxyethylene Sulfate (Stepan Co., USA) with concentration 0.33% g/g, Cocoamidopropyl Betaine (Goldschmidt, Germany) with concentration 0.17% g/g and Glycerol (Fluka, anhydrous p.a. 99.5% GC). The chemicals are dissolved in water (millipore milli-Q) as in [17]. The glycerol concentration is varied between 40% g/g and 60 % g/g to change the bulk viscosity η of the foaming solution. SLES foam of the same gas volume fraction as Gillette foam, $\phi=(93.0\pm0.5)\%$, is produced by simultaneously flowing the SLES solution and pressurized nitrogen gas through a glass bead column [18].

To characterize the foam structures we inject samples between two horizontal parallel glass plates held at a distance of 5 mm, a geometry similar to that of the rheometer. Using video microscopy, we measure the average outer diameter of the dark contour around about 500 bubbles near the top and 500 bubbles near the bottom plate. We thus determine versus foam age the average of the bubble size distribution d and its standard deviation normalized by d, denoted μ_2. Since the coarsening speed depends on gas volume fraction, significant drainage can be ruled out as long as d and μ_2, obtained at the top and bottom plates, coincide within experimental accuracy. This criterion holds for all our samples over the range of foam ages where we perform rheological measurements. Under these conditions μ_2 remains constant at a value of 0.60 ± 0.05 for both Gillette and SLES foams. Moreover, over the duration of a frequency sweep, d always remains constant within $\pm10\%$. To check that the bubbles in contact with the glass plate age in the same way as those deep in the bulk, we measure the transmitted diffuse light intensity through a Gillette sample. This measurement yields the optical transport mean free path in the foam, l^*, which is proportional to the bulk average bubble size [19]. The comparison between videomicroscopy and optical data shows that the ratio of d/l^* does not evolve by more than $\pm5\%$ over the range of foam ages studied in our rheological measurements. We finally note that only the *relative* evolution of d with time, for each foam, matters in the following analyses. Therefore we do not take into account the constant factor relating d to the true average bubble diameter [20]. All the rheological and optical measurements are performed at $(21\pm1)\,^{\circ}$C.

III. RESULTS

The variations of G^* with frequency and bubble size are shown in Fig. 1. All the data obtained both in the rigid and mobile cases (including data with other glycerol concentrations that are not shown) have several features in common: $G'(f)$ converges at low frequency to a plateau, corresponding to the modulus G. Moreover, as frequency is increased by two decades, the evolution of G' is small, but the loss modulus G'' grows almost by an order of magnitude. For a given bubble size, the prediction given by Eq. (2) can be fitted to the evolutions of both $G'(f)$ and $G''(f)$ with frequency, in the range between 2 and 80 Hz, by adjusting G, f_c and η_∞. We do not extend the fits to frequencies below 2 Hz, because in this range well identified slow processes not modeled by Eq. (2) have been shown to be dominant [2,3,8,9], as mentioned

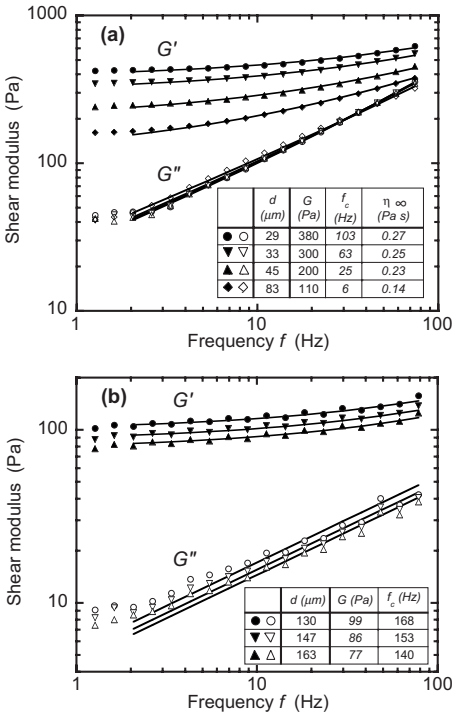

FIG. 1. Elastic G' and loss G'' shear moduli of foams with (a) rigid interfaces (Gillette) or (b) mobile interfaces (SLES-60% glycerol). For each bubble diameter, the lines correspond to fits of Eq. (2) to the respective G' and G'' data. In the mobile case (b), η_∞ is found to be zero. The error bars are of the order of the symbol sizes.

in the introduction. Figure 1 reveals a major difference between foams with either rigid or mobile interfaces: Indeed, the respective anomalous dissipations differ by an order of magnitude for comparable bubble size and surface tension, at given gas volume fraction. This new result demonstrates that interfacial physico-chemistry has a major impact on macroscopic foam viscoelasticity.

IV. DISCUSSION

To explain these findings we first recall the dominant microstructure changes that occur when foam is sheared [cf. Figure 2(a)]. Some films become longer, others shorter, leading to bulk viscous friction in the films and in the liquid channels where these films join, called Plateau borders. Macroscopic shear also compresses or dilates the liquid-gas interfaces, inducing dissipation due to interfacial surface viscosity. The effective viscosity arising from these local processes has been predicted using a scaling approach by Buzza *et al.* [11], but its connection with the mesoscopic model Eq. (2) was so far unclear. We provide this link by identifying the relaxation frequency f_c in Eq. (2) with those that we calculate for the local processes, as we shall now describe.

For rigid interfaces, Marangoni flow in the films is predicted to dominate the dissipation: Shear induces changes of the film areas that modulate the local surfactant concentrations. This leads to surface tension gradients, in proportion to the surface elastic modulus E_s, which drive surfactant transport along the interfaces. Figure 2(a) illustrates that for films perpendicular to the shear direction, these surfactant flows are of opposite direction on opposite film surfaces, inducing bulk shear flow and viscous dissipation within the film. This process yields a contribution to the effective viscosity η_{eff} that scales as the bulk foaming liquid viscosity η multiplied by a strain concentration factor d/δ, as previously considered [4]. However, an additional contribution to η_{eff} arises from the interfacial viscous resistance. It scales as surface viscosity κ multiplied by the specific surface $\sim 1/d$, leading to the prediction [11]: $\eta_{eff} \propto \eta d/\delta + \kappa/d$. Furthermore, since the relaxation process considered here is driven by surface elasticity, the modulus g in Eq. (3) scales as [11]: E_S/d. On this basis, we predict the relaxation frequency f_c:

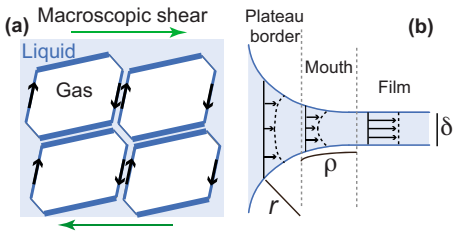

FIG. 2. (Color online) Interfacial and bulk flow in foam subjected to oscillatory shear [11]. a) Marangoni flow in the films of a foam with rigid interfaces schematically represented as a two-dimensional hexagonal structure. Stretched (compressed) interfaces with enhanced (reduced) surface tension are indicated by thick (thin) lines. The black arrows illustrate the surfactant motion at the interfaces. b) Marginal regeneration flow out of a Plateau border with mobile interfaces. The arrows schematically represent the velocity profile.

$$f_c \propto \frac{E_S}{\eta d^2/\delta + \kappa}. \tag{4}$$

In the case of mobile interfaces, dissipation is dominated by marginal regeneration flows at the junction between Plateau borders [cf. Figure 2(b)]: When a foam is sheared, films are lengthened or shortened as liquid is withdrawn from or recedes into Plateau borders. The dilatation of the interfaces is concentrated in the dynamical "mouth," of extent ρ where the films of thickness δ join the Plateau borders. The effective viscosity of the foam is in this case predicted to scale as $\eta_{eff} \propto \eta + \kappa/\rho$, where the additional contribution κ/ρ is due to interfacial stretching in the mouth region [11]. The marginal regeneration flows are driven by the capillary pressure T/r in the Plateau borders whose radius of curvature is denoted r. This leads to a storage modulus [11]: $g \propto T/r$ and a scaling: $f_c \propto (T/r)/(\eta + \kappa/\rho)$. Since for a given gas volume fraction we have [21,22] $\rho \propto r$ and $r \propto d$, we finally predict

$$f_c \propto \frac{T}{\eta d + \kappa}. \tag{5}$$

To discriminate between the mechanisms respectively leading to Eqs. (4) and (5), we study how the experimentally determined relaxation frequency f_c scales with bubble size. In view of Eq. (1), this is equivalent to studying the variation of f_c with G, which is predicted as follows:

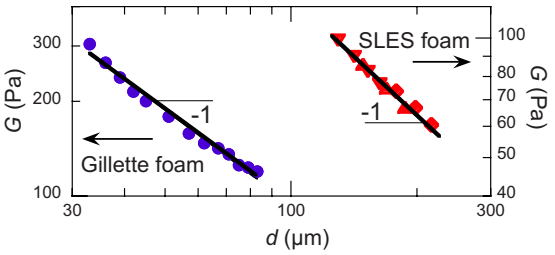

FIG. 3. (Color online) Shear modulus G versus average bubble diameter d, for Gillette shaving foam, and SLES foams: (♦) 40% glycerol, (▲) 50% glycerol, and (▼) 60% glycerol. The straight lines are fits of Eq. (1).

$$f_c \propto \frac{G^2}{A_r + B_r G^2} \quad \text{rigid case} \tag{6}$$

with the parameters given by

$$A_r \propto \eta T^2/\delta E_s \tag{7}$$

and

$$B_r \propto \kappa/E_s. \tag{8}$$

In the mobile case, f_c is predicted as

$$f_c \propto \frac{G}{A_m + B_m G} \quad \text{mobile case} \tag{9}$$

with the parameters

$$A_m \propto \eta \tag{10}$$

and

$$B_m \propto \kappa/T. \tag{11}$$

According to our predictions Eqs. (6) and (9), in the mobile case f_c/G is a monotonously decreasing function of G whereas in the rigid case f_c/G goes through a maximum for:

$$G_{\max} = \sqrt{A_r/B_r} = \sqrt{\eta T^2/(\delta\kappa)} \tag{12}$$

For all data sets, we obtain f_c and G by fitting Eq. (2). Figure 3 shows that for both types of foam G scales with d as predicted by Eq. (1), in agreement with previous results [10]. The plot f_c/G versus G shown in Fig. 4 reveals very different scalings that are robust signatures of different local dissipation processes, controlled by interfacial rigidity. For Gillette foam, we observe an increase $f_c/G \propto G$, which can be fitted only by Eq. (6) and not by Eq. (9), in full agreement with our predictions in the rigid case. Moreover, these data indicate that G_{max} must be much larger than the experimentally investigated range of shear moduli. The fit yields: $A_r = (1663 \pm 77)$ Pa^2 s^{-1} and $0.0000 < B_r < 0.0007$ s^{-1}, so that $G_{max} > 1500$ Pa and the contribution of the surface viscosity κ to the dissipation is negligible compared to that due to the bulk viscosity η.

For the SLES foams, Fig. 4 shows that f_c/G decreases with G, in agreement with our prediction for the mobile case Eq. (9). A decrease of f_c/G with increasing G could be described by Eq. (6) only if for these foams, G_{max} were below the investigated range of shear moduli, close to 60 Pa. In

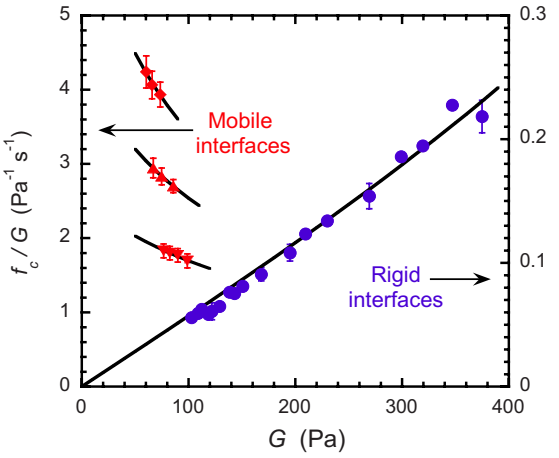

FIG. 4. (Color online) Scaled characteristic frequency f_c/G of the collective bubble relaxation mode versus the elastic modulus G: (●) Gillette shaving foam, (♦) SLES–40% glycerol, (▲) SLES–50% glycerol, and (▼) SLES-60% glycerol foams. The continuous lines represent fits of Eqs. (6) and (9), respectively, for the rigid and mobile cases. We use least square fits with a level of confidence of 95% and equal weight to each data point. Unless indicated, the error bars are smaller than the symbol sizes.

view of Eq. (12) and our result for Gillette foam ($G_{max} = 1500$ Pa), this means that the ratio $\eta T^2/(\delta\kappa)$ would have to be more than 400 times smaller for SLES foams compared to Gillette foam. Using the data for η, T and κ given in Table I, we find that, the equilibrium film thickness δ in SLES foams would have to be more than four orders of magnitude larger than in Gillette foam. Since δ is typically in the range of 10–100 nm, this would mean that SLES films have an equilibrium thickness larger than 100 μm, which is unphysical. We therefore conclude that only Eq. (9) can explain the data measured for the SLES foams shown in Fig. 4, as predicted by our analysis of the mobile case.

Furthermore, the fits show that A_m and B_m depend on the glycerol concentration of the foaming solution. Since the geometrical prefactors in Eq. (9) are not predicted, A_m and

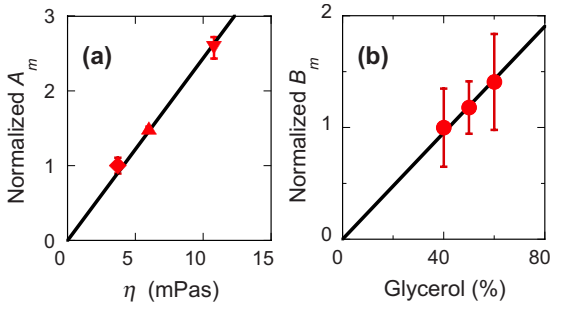

FIG. 5. (Color online) a) Normalized A_m [defined in Eq. (10)] versus bulk viscosity η of the foaming solution, for foams with mobile interfaces: (♦) SLES–40% glycerol, (▲) SLES–50% glycerol, and (▼) SLES-60% glycerol foams. The straight line represents Eq. (10). b) Normalized B_m [defined in Eq. (11)] versus glycerol concentration.

B_m are normalized by their values for the SLES-40%glycerol foam: $A_m=(0.15\pm0.02)$ Pa s and $B_m=(0.0014\pm0.0002)$ s. Figure 5(a) shows a strong linear correlation of A_m with the bulk solution viscosity η determined from independent measurements, in full agreement with Eq. (10) and the discussion above. Figure 5(b) shows a small increase of B_m with the amount of glycerol, consistent with previous measurements of interfacial shear viscosity [23]. However, B_m and κ are hard to compare quantitatively, in view of the uncertainty on the measurements in this low range of κ. In further studies, it would be interesting to probe a broader range of interfacial rigidities, using other surfactant solutions. For instance, the addition of a fatty acid is known to rigidify the interfaces (Examples are given in [14]). However, the lack of stability of these solutions prevented us so far from using them to make foams with the generator described above. It would also be interesting to extend our study to higher strain amplitudes where the film thickness may increase significantly, as suggested by recent experimental studies [24].

V. CONCLUSION

Our results offer pioneering insight into the physicochemical processes that determine fast macroscopic relaxations in foams. Depending on the rigidity of the gas-liquid interfaces the dominant dissipative process is localized in different elements of the foam structure. Rigid interfaces enhance foam dissipation due to Marangoni flows in the soap films whereas for mobile interfaces dissipation is weaker and due to viscous flow in the borders between the films. These processes set the elementary relaxation time scale. Our findings establish the missing link between rheology on the film scale, mesoscopic collective relaxations, and macroscopic foam viscoelasticity.

ACKNOWLEDGMENTS

We thank N. Denkov for fruitful discussions. H. Sizun provided crucial technical help. We gratefully acknowledge financial support from E.S.A. (MAP No. AO99-108: C14914/02/NL/SH).

[1] P. Sollich, F. Lequeux, P. Hébraud *et al.*, Phys. Rev. Lett. **78**, 2020 (1997).
[2] A. D. Gopal and D. J. Durian, Phys. Rev. Lett. **91**, 188303 (2003).
[3] S. Cohen-Addad, R. Höhler, and Y. Khidas, Phys. Rev. Lett. **93**, 028302 (2004).
[4] A. J. Liu, S. Ramaswamy, T. G. Mason, H. Gang, and D. A. Weitz, Phys. Rev. Lett. **76**, 3017 (1996).
[5] C. Derec, G. Ducouret, A. Ajdari, and F. Lequeux, Phys. Rev. E **67**, 061403 (2003).
[6] R. Höhler and S. Cohen-Addad, J. Phys.: Condens. Matter **17**, R1041 (2005).
[7] H. M. Princen and A. D. Kiss, J. Colloid Interface Sci. **112**, 427 (1986).
[8] S. Vincent-Bonnieu, R. Höhler, and S. Cohen-Addad, EPL **74**, 533 (2006).
[9] S. Besson, G. Debrégeas, S. Cohen-Addad, and R. Höhler, Phys. Rev. Lett. **101**, 214504 (2008).
[10] S. Cohen-Addad, H. Hoballah, and R. Höhler, Phys. Rev. E **57**, 6897 (1998).
[11] D. M. A. Buzza, C.-Y. D. Lu, and M. E. Cates, J. Phys. II France **5**, 37 (1995).
[12] K. J. Mysels, K. Shinoda, and S. Frankel, *Soap Films: Studies of their Thinning* (Pergamon Press, London, 1959).
[13] S. A. Koehler, S. Hilgenfeldt, and H. A. Stone, Langmuir **16**, 6327 (2000).
[14] N. D. Denkov, S. Tcholakova, K. Golemanov *et al.*, Soft Matter **5**, 3389 (2009).
[15] C. Macosko, *Rheology, Principles, Measurements And Applications* (Wiley-VCH, New York, 1994).
[16] G. Bohme and M. Stenger, J. Rheol. **34**, 415 (1990).
[17] K. Golemanov, N. D. Denkov, S. Tcholakova *et al.*, Langmuir **24**, 9956 (2008).
[18] F. Rouyer, S. Cohen-Addad, M. Vignes-Adler, and R. Höhler, Phys. Rev. E **67**, 021405 (2003).
[19] M. U. Vera, A. Saint-Jalmes, and D. J. Durian, Appl. Opt. **40**, 4210 (2001).
[20] A. van der Net, L. Blondel, A. Saugey *et al.*, Colloids Surf., A **309**, 159 (2007).
[21] D. A. Reinelt and A. M. Kraynik, J. Colloid Interface Sci. **132**, 491 (1989).
[22] D. Weaire and S. Hutzler, *The Physics of Foams* (Clarendon Press, Oxford, 1999).
[23] O. Pitois, C. Fritz, and M. Vignes-Adler, Colloids Surf., A **261**, 109 (2005).
[24] J. Emile, E. Hardy, A. Saint-Jalmes *et al.*, Colloids Surf., A **304**, 72 (2007).